Available online at www.sciencedirect.com

ScienceDirect

Procedia CIRP 18 (2014) 144 – 149

www.elsevier.com/locate/procedia

International Conference on Manufacture of Lightweight Components – ManuLight2014

Thermo-mechanical behavior and material failure of steel wire reinforced aluminum

A. Morasch[1]*, M. Wedekind, D. Matias[1], H. Baier[1]

[1] Institute of Lightweight Structures, TU München, Germany

* Corresponding author. Tel.: +49 (0) 89 289 16097; fax: +49 (0) 89 289 16104 *E-mail address*: morasch@llb.mw.tum.de

Abstract

Extruded steel wire reinforced aluminum is a novel, discretely reinforced metal matrix composite. Variation of the wire volume content can alter the mechanical properties, particularly stiffness and strength. Introduced by the compound extrusion process, thermally induced residual stresses affect the mechanical properties and need to be taken into account. Homogenization approaches and a mode-based failure criterion are presented to describe the wire reinforced aluminum efficiently for computational strength analysis. Further, assessing the material´s behavior subjected to impact loads, the material is described with regards to high plastic strains and strain rates, material failure and fracture at complex stress states. The material model is calibrated based on experimental testing and validated by a three-point bending test of an extruded, reinforced section, showing good agreement between experimental and simulated force-displacement curves as well as in fracture patterns.

*Keywords:*steel wire reinforced aluminum; MMC; failure; fracture; maximum shear stress criterion

1. Introduction

In the collaborative research project SFB/ Transregio10, an extrusion process for composite sections is being investigated. One application is the integration of steel wires as reinforcement to an aluminum matrix of extruded sections. By introducing the wires, mechanical properties such as stiffness and strength can be adjusted locally allowing for tailored reinforcements. For an application of the material in load-bearing structures, its orthotropic stiffness and strengths must be known. Stiffness and strength are affected by thermally induced residual stresses that arise by joining steel wires and aluminum matrix at high temperatures and have to be taken into account.

In the second chapter, the mechanical properties of steel wire reinforced aluminum (shown in Figure 1) are discussed for a wire content of 2% with respect to residual stresses. For efficient computational analysis, a homogenized shell-model of the material is presented.

Using high-strength steel wires as reinforcements of a ductile aluminum matrix, the reinforced aluminum offers significantly increased strength in wire direction while maintaining good ductility. This aspect shows potential for the application in crash energy absorbing structures. A material model including the description of material fracture is derived and tested in a three-point bending test of reinforced, rectangular sections (Figure 7).

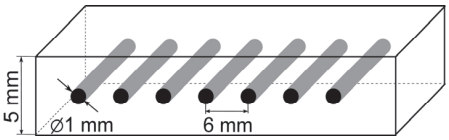

Fig. 1 Hybrid material with wire volume content of 2%

2. Thermo-elastic properties of steel wire reinforced aluminum

The elastic properties of steel wire reinforced aluminum are strongly influenced by the wires. The wires have a stiffening effect, although, they introduce residual stresses due to a difference in coefficients of thermal expansion (CTE). Simulations of the material

doi:10.1016/j.procir.2014.06.122

subjected to a thermal load as in the extrusion process followed by a mechanical loading allow for an assessment of stiffness and yield strength with respect to residual stresses. This methodology is described in the following and verified with experiments.

2.1. Thermo-elastic properties of the constituents

As an input for analyses, the elastic properties and the (CTE) of aluminum matrix and steel wire are needed. Exemplary, a ductile aluminum alloy (EN-AW 6060) and high-strength steel wires (X10CrNi17-7) are chosen. Matrix and wire were tested in tensile tests, giving the elastic properties listed in Table 1. For that, test specimens for the aluminum matrix were cut from extruded flat bars having the same geometry and temper condition (F22) as the reinforced bars, meaning that no special tempering was performed.

Table 1 Properties of aluminum matrix and steel wire

Property	Steel wire	Aluminum
Young´s modulus E in MPa	214000	64700
Poisson´s ratio	0.3	0.3
Yield strength $R_{p0.2}$ in MPa	1900	84
Tensile strength R_m in MPa	2050	148

The CTE were determined in a dilatometer up to a temperature of 150°C. Although this is much lower than the extrusion temperatures (450…550°C), it is close to the Debye temperature where the CTE saturates to a constant value. The determined mean values of the CTE for the processing temperature interval are as follows:

- CTE steel wire = $15 \cdot 10^{-6}$ 1/K
- CTE aluminum matrix = $24.2 \cdot 10^{-6}$ 1/K

2.2. Influence of thermally induced residual stresses on stiffness and yield strength

In order to assess the effect of residual stresses on stiffness and yield strength, finite element simulations are carried out. In a first step, a simulation model of a flat bar of the hybrid material is cooled down with a homogeneous decrease in temperature ΔT, simulating cooling after extrusion. In a second step, a tensile test of the bar with inherent residual stresses is simulated. By comparing simulated and experimental force-elongation data, ΔT is varied until the data shows good agreement as in Figure 2a.
The determined ΔT is then regarded as an equivalent cooling, leading to residual stresses that are comparable to the actual residual stresses in magnitude and distribution (Figure 2b). Neutron scattering experiments determining the residual stresses in the aluminum matrix agree well with the simulated stresses [1]. Whilst the wire is compressed at longitudinal stresses of about 700MPa, the matrix has to bear a high tensile stress and plastifies partially around the wire at 90MPa.

The exemplary force-elongation curve from tensile tests in Figure 2a shows three distinct regions. In region I, wire and matrix deform elastically. In region II, the matrix plastifies with the wire still behaving elastically. In region III, wire and matrix both deform plastically. Taking residual stresses into account, the simulated force-elongation curve matches well with the experimental one with ΔT=-450K. The equivalent cooling is lower than the actual cooling (ΔT≈525°C), because lower material strengths at high temperatures are not considered. Comparing the experimental stress-strain curve to a simulated one without residual stresses shows that once matrix and wire behave plastically, the residual stresses are released and region III is almost unaffected.

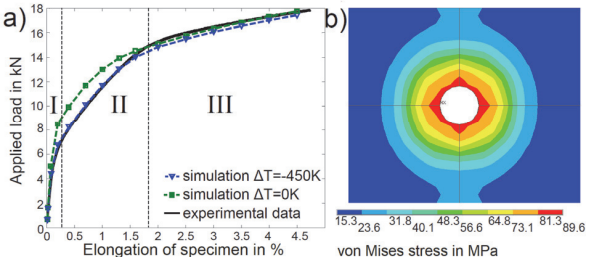

Fig. 2a) Effect of residual stresses on the material´s strain hardening
b) Stress distribution around the wire

2.3. Homogenization approaches for wire reinforced aluminum

The mechanical properties of wire reinforced aluminum are globally anisotropic and locally inhomogeneous. Due to the inhomogeneity and a three-dimensional stress state around the wires, only a simulation model with both wire and matrix discretized with volume elements allows for micromechanical analysis. However, on a structural level, information on structural stiffness and strength do not require a detailed modeling. Models with different levels of are as follows (in order of computational efficiency)

1. Shell-beam-model
2. Homogenized-shell-model
3. Homogenized-beam-model

2.4. Failure model for the homogenized-shell-model

For structural strength analysis, the transition from elastic to plastic behavior is one criterion for failure.
The reasons for plastic material behavior are here:

- Plastification of the matrix (Mode 1)
- Plastification of the wire (Mode 2)
- Debonding of the wire (Mode 3)

A mode-based failure criterion taking into account these failure modes has been developed [2]. Depending on the mechanical properties of wire, matrix and interface, different modes can initiate failure. Mode 1 failure for an isotropic matrix can be simply described by the von Mises yield criterion. With the inherent residual stresses, the matrix is prestressed, leading to orthotropic strengths. Approximating the orthotropic yield strengths, the Tsai-Hill yield criterion [3] was chosen for the description of matrix failure and the effort is as follows

$$Eff_{matrix} = \left(\frac{\sigma_{||}}{\sigma_{||,\max}}\right)^2 + \left(\frac{\sigma_{\perp}}{\sigma_{\perp,\max}}\right)^2 - \frac{\sigma_{||}\sigma_{\perp}}{\sigma^2_{||,\max}} + \left(\frac{\tau_{\perp||}}{\tau_{\perp||,\max}}\right)^2 . \quad (1)$$

At pure tension in wire direction, a low yield strain of the wire can initiate plastic behaviour:

$$Eff_{wire} = \left(\frac{\varepsilon_{||,wire}}{\varepsilon_{||,wire,\max}}\right)^2 . \quad (2)$$

Debonding of the interface mainly occurs due to normal tensile stresses at the interface. Therefore, the effort of the interface is

$$Eff_{Interface} = \left(\frac{\sigma^{+}_{\perp}}{\sigma_{Interface,\max}}\right)^2 . \quad (3)$$

As the failure modes describe the onset of plasticity, there is apparently no interaction between them and the complete failure criterion is

$$Eff_{total} = \max\left(Eff_{matrix}; Eff_{wire}; Eff_{Interface}\right). \quad (4)$$

3. Strain hardening and fracture of steel wire reinforced aluminum

For high plastic strains (ε_p>0.3) as typically occurring during impact processes, residual stresses play only a minor role. A high energy absorption can be reached with high flow stresses. Due to the high yield strength of the wires, the flow stresses of the reinforced aluminum in wire direction are increased significantly already at low wire volume contents [2]. Radially supported by the aluminum matrix, necking is postponed and low fracture strains (ε_f=1.8%) of the wires are increased to axial strains of about 20%. Increased flow stresses makes steel wire reinforced aluminum interesting for energy absorption for load cases with dominating tension in wire direction. As the strain hardening information from tensile tests is limited to the ultimate strain at necking (ca. 1.8% for the wire, 20% for the aluminum matrix), strain hardening data has to be extrapolated.

3.1. Extrapolation of the material´s strain hardening

An extrapolation function offering a saturation stress should be chosen, as the strain hardening function of most aluminum alloys is known to saturate. A good fit to the experimental data is obtained using the Hockett-Sherby function [4] (Figure 3).

σ_y is the uniaxial yield strength, σ_S, p and N are fitting parameters

$$\sigma = \sigma_S - \left(\sigma_S - \sigma_y\right)\cdot \exp\left(-\left(N\cdot\varepsilon\right)^p\right). \quad (5)$$

The quality of the extrapolated strain hardening curve can be improved by introducing Considère´s criterion [5] to the fitting procedure. Considère´s criterion states that necking in uniaxial tension sets in at maximum force and thus provides additional knowledge to the fitting procedure. Translated into the regime of true stresses and true strains, Considère´s criterion is

$$\frac{d\sigma}{d\varepsilon}|_{\varepsilon=\varepsilon_u} = \sigma\left(\varepsilon_u\right). \quad (6)$$

This can be introduced to the fitting as a set of two constraints

$$\left|\frac{d\sigma^{fit}}{d\varepsilon}|_{\varepsilon=\varepsilon_u} - \sigma^{fit}\left(\varepsilon_u\right)\right| - \delta_1 \le 0 \quad (7)$$

$$\left|\sigma^{\exp}\left(\varepsilon_u\right) - \sigma^{fit}\left(\varepsilon_u\right)\right| - \delta_2 \le 0 . \quad (8)$$

Constraint (7) ensures that at the point of ultimate strain, Considère´s criterion is fulfilled within a certain limit δ_1. Constraint (8) ensures that the ultimate stress of the fitted function equals the experimental ultimate stress within the limit δ_2. Tensile tests of the high-strength steel wires were performed giving values of Table 1. Due to low plastic hardening capabilities, it is reasonable to model the wire as elastic-perfectly-plastic.

3.2. Strain rate hardening

During impact processes, strain rates in highly loaded regions can be as high as several $\dot{\varepsilon}$ =100 1/s. If a material exhibits a strain rate sensitive strain hardening, this has a non-negligible influence on the structural response. However, most aluminum alloys only show little strain rate sensitivity which can often be neglected. A similar aluminum alloy EN AW-6082 (T4) was tested in a high speed tensile testing machine at different strain rates (done by IAM–Karlsruher Institut für Technologie). The strain hardening curves in Figure 3 confirm a small strain rate dependence, which is considered negligible for further research.

Experimental data for steel wires is not available for high strain rates. However, tests of similar high-strength steel alloys suggest, that strain rate effects are small and can also be neglected [6].

4. Modeling of failure and fracture

Modeling the material´s failure and fracture, the

forming limits of the matrix are used as a criterion for onset necking as ductile failure. In order to also cover shear dominated fracture, the maximum shear stress criterion is used. For the thin wires with mostly uniaxial tension stresses, a maximum strain criterion is used. Also failure of the interface (e.g. wire debonding) can accelerate the fracture process and needs to be assessed.

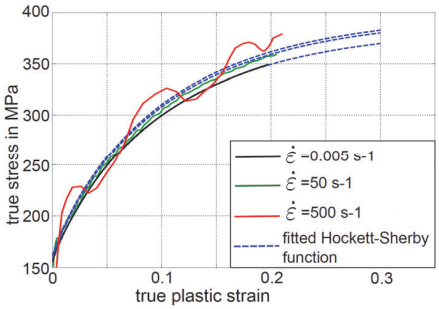

Fig. 3 Strain rate dependent strain hardening of EN-AW 6082 T4

4.1 Fracture model for the aluminum matrix based on forming limits and the maximum shear stress criterion

Strain state dependent forming limits are determined with a simulation model of an aluminum sheet, which is stretched at different global strain ratios (Figure 4). Necking is determined, once the maximum strain rate in thickness direction in the model exceeds the minimum strain rate by a factor beta

$$\beta = \frac{\dot{\varepsilon}_{3,\max}}{\dot{\varepsilon}_{3,\min}}. \quad (9)$$

Choosing the value for beta too high results in overpredicted forming limits, choosing beta too close to unity, small strain rate fluctuations in the model are misinterpreted as necking. With beta=2, necking was determined shortly after onset.

Forming limits further mainly depend on:

- Strain hardening
- Yield function
- Material and geometric imperfections

The fitted Hockett-Sherby strain hardening function is used for the material model. As it was not possible to assess the orthotropic yield behavior of the reinforced aluminum matrix experimentally, an isotropic yield behavior of the matrix had to be assumed. For this, the isotropic Hershey yield function is chosen, as the von Mises yield criterion is known to overpredict the forming limits, mainly at biaxial strain states. The Hershey yield function is [7]

$$\Phi = \left|\sigma_1 - \sigma_2\right|^m + \left|\sigma_2 - \sigma_3\right|^m + \left|\sigma_3 - \sigma_1\right|^m = 2\sigma_y \quad (10)$$

The yield exponent m is related to the lattice structure and is chosen as m=8 for face-centered-cubic aluminum. Material and geometric imperfections are modeled as a statistical variation of the sheet thickness following a Gaussian distribution, which was first suggested by Lademo [8]. The magnitude of the difference in sheet thickness Δt is calibrated according to the necking strain from uniaxial tensile test giving Δt=0.0025t. The standard deviation σ is chosen as 3σ=Δt. The so determined necking strains are shown in Figure 5 and are implemented into the simulation program LS-DYNA as Müschenborn and Sonne forming limits in order to account for failure accumulation at non-linear strain paths [9].

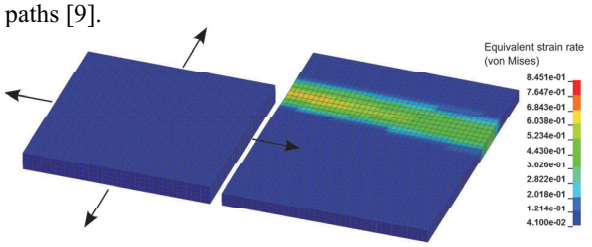

Figure 4 Simulation model for the determination of forming limits stretched at a global strain ratio of $\varepsilon_{min}/\varepsilon_{maj}$=1/4

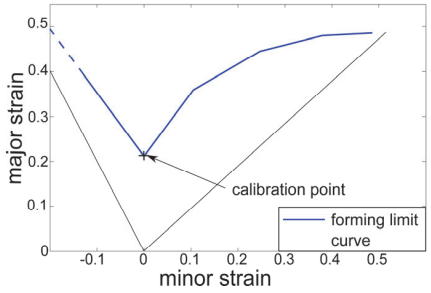

Figure 5 Simulated forming limit diagram with calibration point from tensile test

4.2 Evolution of necking failure

Especially thick sheet has a high remaining forming capability after onset of necking, which does not lead to sudden fracture. Thus, the forming limits are used as a criterion for onset of failure, which evolves according to a failure evolution until final fracture. The applied failure evolution was proposed by Borvall et al [10] and is available in LS-DYNA. After onset of failure, the failing element is degraded by

$$\sigma = \left(1 - D\right) \cdot \tilde{\sigma}. \quad (11)$$

σ is the degraded stress, D the damage parameter and $\tilde{\sigma}$ is the undamaged true stress. The damage rate is linked to the plastic displacement of the failing element and evolves according to

$$\dot{D} = \frac{l\dot{\varepsilon}^p}{u_f^p}. \quad (12)$$

Length l is the characteristic element length, thus making the failure evolution element size dependent. The ultimate plastic deformation u_f^p after onset of failure is chosen as u_f^p=0.3 taking into account the high

remaining deformation capability of the thick aluminum matrix after onset of necking.

4.3 Maximum shear stress criterion

Describing material failure by using forming limits only covers stress states of triaxialities in the range of $0.33<\eta<0.66$. For low triaxialities, fracture is mainly dominated by shear fracture. For this reason, the maximum shear stress criterion is chosen as fracture criterion. Assuming plane stress conditions, it is

$$\tau_{\max} = \left\{ \frac{\sigma_1 - \sigma_2}{2}; \frac{\sigma_2}{2}; \frac{-\sigma_1}{2} \right\} = \tau_{fail} \,. \tag{13}$$

This can be translated into a strain state dependent fracture strain [11] using the Hollomon strain hardening function (fitted to experimental strain hardening data)

$$\bar{\varepsilon}_f = C \left\{ \frac{\sqrt{1+\alpha+\alpha^2}}{2+\alpha} \right\}^{1/n} \quad for \; -\frac{1}{2} < \alpha < 1 \tag{14a}$$

$$\bar{\varepsilon}_f = C \left\{ \frac{\sqrt{1+\alpha+\alpha^2}}{1-\alpha} \right\}^{1/n} \quad for \; -2 < \alpha < -\frac{1}{2}. \tag{14b}$$

α is the strain ratio $\varepsilon_{min}/\varepsilon_{maj}$, and n is the Hollomon hardening exponent. The calibration constant C is defined from the fracture strain of a shear test of a flat shear specimen shown in Figure 6, which provides a stress state close to pure shear [12]. For shear fracture, the same evolution functions are used as for necking failure, yet with a lower ultimate deformation after onset of fracture $u_f^p=0.1$ in order to account for crack growth through the fracturing element.

4.4 Maximum strain criterion for the steel wires

For thin steel wires and mostly tension in wire direction, a fracture criterion according to the maximum plastic strain in the wire is chosen

$$\bar{\varepsilon}_f = \varepsilon_{p,\max} \,. \tag{15}$$

The fracture strain was taken from the tensile tests of the reinforced aluminum as $\varepsilon_{p,\max} = 0.22$.

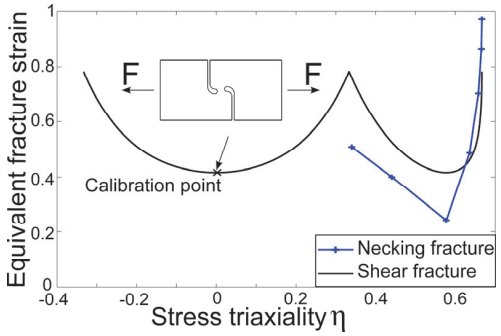

Figure 6 Shear specimen and fracture strains predicted from maximum shear stress criterion and from simulated forming limits

4.5 Interface failure

For failure and fracture of the hybrid material, interface failure can be severe. Especially at tension perpendicular to the wire direction, widely different strengths of wire and aluminum matrix lead to early debonding of the wire. This creates a hole in the matrix reducing the load bearing cross-section and provoking early fracture of the matrix.

For uniaxial tension in wire direction, the plastic flow ratios of wire and matrix are equal due to volume conservation. Thus, no normal stresses arise in the interface that could lead to interface failure (until necking of the matrix). Push-out tests showed that the interface´s shear strength is sufficient enough in order to use the full strength of the wire [13]. Micrographs of tensile specimens at different elongations confirm, that wire debonding starts after the matrix begins to neck [13], so that for dominating tension in wire direction, interface failure plays a minor role.

5. Validation of the material model

After calibrating the fracture models, the material model is validated. As the material is assumed as insensitive to a change in strain rate, a quasi-static three-point bending test of a reinforced extruded section was done, providing a complex stress state, superimposing bending and shear loads. Additionally, a hole was milled into the sections in the symmetry line of the bending-punch as shown in Figure 7, triggering fracture.

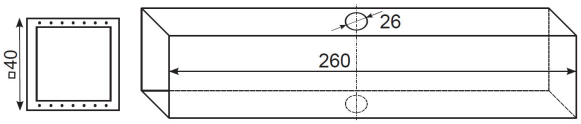

Figure 7 Reinforced specimen for three-point bending

5.1 Comparison of simulated and experimental bending test

Comparing experimental and simulated force-displacement curve in Figure 8b shows a good agreement until peak force. At this force, the matrix has to bear high strains ($\varepsilon_p>0.3$), so that matching the experimental maximum force argues for the determined strain hardening extrapolation.

Figure 8a shows simulated and experimental principal strain in the side of the section and fracture at a punch displacement of 25mm. The section´s deformation and the strain distribution agree reasonably well. Yet, the fracture evolution is underpredicted with ductile fracture first running along one side of the section and the second side fracturing too late. This results in an overpredicted

strength of the fracturing section as can be seen in Figure 8b.

5.2 Discussion of the modeling technique

Simulating wire reinforced aluminum with a shell-beam model is able to reproduce the mechanical behavior of reinforced sections for the given bending test. With a good prediction of material fracture, the fracture model based on simulated forming limits and the maximum shear stress criterion is suitable.
However, this modeling technique is limited to following cases:

- fracture is dominated by fracture of the matrix
- debonding of the wires does not occur for the given load case, or has negligible influence
- the structure can be approximated with shell elements

With regards to these limitations, the chosen validating example with 5mm thickness and the given section dimensions, puts the modeling technique to its limitations. However, good results were obtained.

For sections and load cases where the assumptions do not apply, a simplified shell-beam model is not valid. Then, a detailed volume model has to be used which also takes interface failure into account.

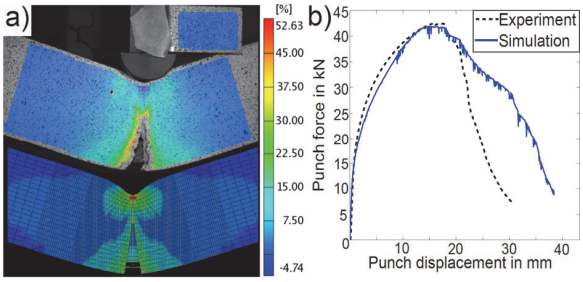

Figure 8a) Principal strain distribution from simulation and optical measurement and fracture at a punch displacement of 25mm
8b) Force-displacement curves from experiment and simulation

6. Conclusion

Steel wire reinforced aluminium is a promising material as its stiffness and strength can be varied in a wide range, only adding little additional mass by local reinforcements. However, residual stresses lower the yield strength of the material and have to be considered for structural analysis. For this purpose, a simulation technique for the prediction of thermally induced residual stresses is presented. Homogenizing the reinforced aluminum and modeling it with shell elements allows for efficient structural analysis. A mode based failure criterion can be used for the prediction of failure as onset of plasticity [2].

For the prediction of fracture, a material model for a shell-beam representation is calibrated and tested in three-point bending tests. The strain hardening properties are determined from tensile tests and extrapolated with a constrained fitting approach.

A fracture model based on forming limits and the maximum shear stress criterion is presented and tested in a three-point bending test of a reinforced section showing good agreement of experiment and simulation. However, possible limitations to the shell-beam model were identified. For these cases, a volume model with a more complex description of fracture (for instance by the Gurson model) and also taking into account interface failure has to be chosen.

Acknowledgements

The research presented in this paper was carried out within the Transregional Collaborative Research Center SFB/Transregio10, subproject C6, which is kindly supported by the German Research Foundation (DFG).

References

[1] F. Zaeh, A. E. Tekkaya, M. Langhorst, M. Ruhstorfer, A. Schober, D. Pietzka, 2009. Experimental and numerical investigation of the process chain from composite extrusion to friction stir welding regarding the residual stresses in composite extruded profiles. Prod. Eng. Res. Devel., Vol. 3, pp. 353-360.
[2] M. Wedekind, 2013. Charakterisierung von Steifigkeit und Festigkeit heterogen verstärkter Verbundstranprofile. Dissertation, Lehrstuhl für Leichtbau, TU München.
[3] S. W. Tsai, 1968. Strength theories of filamentary structures, fundamental aspects of fiber reinforced plastic composites. Wiley-Interscience, New York.
[4] J. E. Hockett, O. D. Sherby, 1975. Large strain deformation of polycrystalline metals at low homologous temperatures. J. Mech. Phys. Solids, Vol. 23, pp. 87-98.
[5] P. Hora, 2006. Advanced constitutive models as precondition for an accurate FEM-simulation in forming applications
[6] B. L. Boyce, T. B. Crenshaw, M. F. Dilmore, 2007. The strain rate sensitivity of high-strength high-toughness steels. Sandia National Laboratories, Sandia Report, SAND2007-0036.
[7] A. V. Hershey, 1954. The plasticitiy of an isotropic aggregate of anisotropic face centered cubic crystals. J. Appl. Mech. – Trans ASME 21, pp. 236-240.
[8] O. G. Lademo, T. Berstad, O. S. Hopperstad, K. O. Pedersen, 2004. A numerical tool for formability analysis of aluminum alloys. Part I: Theory. Steel Grips 2, Suppl. Material Forming.
[9] W. Müschenborn, H. M. Sonne, 1975. Einfluß des Formänderungsweges auf die Grenzformänderungen des Feinbleches. Arch. Eisenhüttenwesen, Vol. 46, pp. 397-602.
[10] T. Borvall, T. Johansson, M. Schill, 2013. A General Damage Initiation and Evolution Model (DIEM) in LS-DYNA. 9th European LS-DYNA Conference.
[11] T. Wierzbicki, Y. Bao, et al, 2005. Calibration and evaluation of seven fracture models. Int. J. Mech. Sci., Vol. 47, pp. 719-743.
[12] J. Peirs et al, 2009. Novel pure-shear sheet specimen geometry for dynamic material characterization. 9th International Conference on the Mechanical and Physical Behaviour of Materials under Dynamic Loadings, DYMAT 2009, pp. 35-41.
[13] M. Meissner, 2010. Experimentelle und CAE gestützte Untersuchung des Schädigungsverhaltens der unidirektional federstahldrahtverstärkten Aluminiumlegierung EN AW.6082 bei variierendem Verstärkungsanteil. Studienarbeit iwk I, KIT Karlsruhe.